# Collisions between Nitrogen-14 and Nitrogen-15 Spin-Labels. 1. Lipid–Lipid Interactions in Model Membranes†

Jean Davoust, Michel Seigneuret, Paulette Hervé, and Philippe F. Devaux*

ABSTRACT: A new method is described to evaluate collision frequencies between spin-labeled molecules in membranes. This method utilizes a mixture of $^{14}N$ and $^{15}N$ nitroxides. The extent of spin–spin interaction between the two different isotopes can be determined by comparing experimental ESR spectra with simulated spectra. The latter are calculated by using modified Bloch equations and by assuming that the spin exchange process is the dominant broadening mechanism. A more approximate analysis is also described; it is based on the evaluation of the line broadening from the measurement of peak heights. Both analyses show that relatively low concentrations of label can be utilized: 1–5% labeled lipids in a membrane give a broadening sufficient to allow quantitation. Collision frequencies equal to or larger than 0.1 MHz can be evaluated by this method. Because of the limited overlap between $^{15}N$ and $^{14}N$ spectra, this method allows the investigation of the collisions between unlike molecules of very different concentration. From the collision frequencies, the topological domain explored by a probe can be inferred as well as its lateral diffusion constant. In this paper, it is shown that in spite of the low order of the chain residues near their methyl terminal, a probe linked at the $\omega - 2$ position of an ionized stearic acid does not interact with a probe positioned near the polar region. Nevertheless the former probe, deeply embedded in the membrane, explores a larger volume. It is also shown that if the nitroxide is attached to a fatty ester, the probe "sees" evenly the whole hydrophobic region of the membrane.

By analysis of the ESR spectra obtained with spin-labeled molecules homogeneously diluted into a membrane, it is possible to determine the order parameter and mobility of a lipid residue embedded within a membrane. [for extensive reviews, see the book of Berliner (1976)]. Such parameters are largely intramolecular and only partially reflect intermolecular interactions. Spin-labels can be used also to determine intermolecular parameters such as average distances, collision rates, and diffusion constants. This requires that the local concentration of spin-label be sufficiently high to produce broadening and line-shape distorsions due to electron spin–electron spin interactions. Empirical approaches of the line broadening have been utilized by several authors to determine lateral diffusion constants and lipid phase diagrams (Devaux & McConnell, 1972; Sackmann & Traüble, 1972a; Hartmann & Galla, 1978; Ohnishi & Tokutumi, 1981). Theoretically the dipole–dipole interaction can be used to determine the proximity of labeled residues in a frozen state (Kokorin et al., 1972), while Heisenberg spin exchange, which is a contact interaction, gives access to collision rates and thus to lateral diffusion constants. One way to obtain quantitative information on the Heisenberg spin exchange rates is spectral simulation using modified Bloch equations (Sackmann & Traüble, 1972b; Scandella et al., 1972; Devaux et al., 1973; Sackmann et al., 1973). More recently Popp and Hyde used ELDOR to determine the extent of Heisenberg spin exchange between spin-labeled fatty acids in a membrane (Popp & Hyde, 1982).

In this and the following paper (Davoust et al., 1983) it will be shown that the accuracy and potential of the method of spin–spin interactions between nitroxides can be extended if nitroxides with different nitrogen isotopes ($^{14}N$ and $^{15}N$) are mixed in the same sample. Collision frequencies between two different species can be investigated unambiguously. By the double-labeling procedure, information can be gathered on proximity relationships betwen unlike molecules. Thus, the topological domains seen by the various labeled residues of a lipid or a protein can be investigated. Simultaneously this technique allows one to estimate lateral diffusion rates in the immediate environment of each probe.

In the first paper, the theoretical background necessary to understand how spectra are analyzed in terms of a spin-exchange frequency is outlined. Simulated spectra are shown, together with experimental spectra obtained with liposomes containing various mixtures of labeled lipids. The advantanges and limitations of the method are discussed through specific examples. The following paper will extend the method to the investigation of lipid–protein specificity (Davoust et al., 1983).

## Materials and Methods

*Spin-Label Synthesis.* Figure 1 represents the various spin-labeled lipids used in this study. The molecule on the left is a $^{15}N$ derivative, while all other molecules (right) are $^{14}N$ derivatives. The nomenclature utilized is that of Hubbell & McConnell (1971). $^{15}N(1,14)FA$[1] and the corresponding methyl ester were synthetized according to Bienvenüe et al. (1978). The final purification step of the ester was performed by high-pressure liquid chromatography (LIREC A 802) using a preparative silica gel column (Lichrosorb) eluted with hexane–chloroform (70:30).

The $^{14}N$-spin-labeled phospholipids (1,14)PC, (10,3)PC, and (0,2)PC as well as the fatty acid (7,8)FA were prepared according to Hubbell & McConnell (1971) and Devaux et al. (1975). Tempolecithin (TL) was synthesized according to

† From the Institut de Biologie Physico-Chimique 13, rue Pierre et Marie Curie, F-75005 Paris, France. *Received December 9, 1982.* This work was supported by grants from the Centre National de la Recherche Scientifique (ERA 690), the Délégation Générale à la Recherche Scientifique et Technique, and the Université Paris VII.

[1] Abbreviations: ESR, electron spin resonance; $^{15}N(1,14)FA$, 16-[$^{15}N$]doxylstearic acid; (1,14)PC, 1-palmitoyl-2-(16-doxylstearoyl)-phosphatidylcholine; (7,8)FA, 10-doxylstearic acid; (10,3)PC, 1-palmitoyl-2-(5-doxylpalmitoyl)phosphatidylcholine; (0,2)PC, 1-palmitoyl-2-(4-doxylpentanoyl)phosphatidylcholine; TL (tempolecithin), 1,2-dipalmitoylphosphatidyltempocholine; doxyl, 4,4-dimethyl-3-oxyoxazolidin-2-yl; tempocholine, *N,N*-dimethyl-*N*-(2,2,6,6-tetramethyl-1-oxypiperidin-4-yl)-*N*-(2-hydroxyethyl)ammonium hydroxide; Hepes, 4-(2-hydroxyethyl)-1-piperazineethanesulfonic acid.

0006-2960/83/0422-3137$01.50/0 

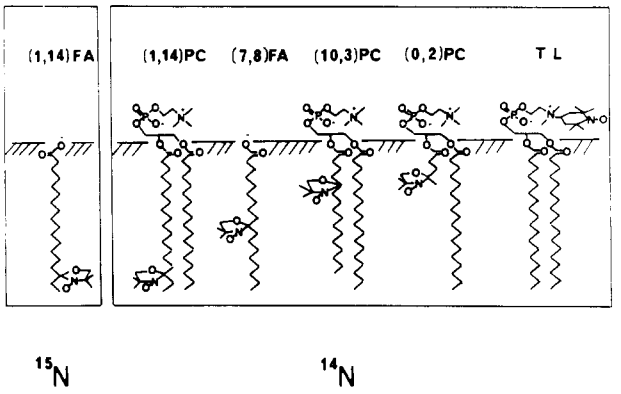


FIGURE 1: Diagrammatic representation of the structures and average membrane positioning of the various spin-labeled lipids used in this study.

Kornberg & McConnell (1971a) from dipalmitoylphosphatidylcholine (Sigma).

*Lipid Sample Preparation.* Egg yolk phosphatidylcholine (lecithin) was extracted according to Singleton et al. (1965). In order to get identical amounts of $^{15}N$ labels, all samples were prepared from aliquots of a lecithin solution in chloroform containing a fixed percentage of the $^{15}N$-spin-labeled fatty acid or ester to which various amounts of $^{14}N$-spin-labeled phospholipids were added. The solvent was then evaporated under argon; 100 mM Hepes, pH 8, carefully degassed, was added to resuspend the dry lipid film.

*ESR Experiments.* ESR spectra were run on a Varian E 109 spectrometer equipped with a field-frequency lock and a temperature control device and interfaced to a Tektronix 4051 computer for data accumulation double integration and storage. All spectra were recorded by using a 100-G scan range and a 0.5-G modulation amplitude. Interaction broadened spectra were also recorded over a 200-G range in order to get a proper determination of the double integral.

*Determination of Spin-Label Concentrations.* After completion of the experiments with membranes, each sample was solubilized with a large excess of sodium dodecyl sulfate (Serlabo), and the ESR spectrum was recorded. All spin–spin interactions being abolished by detergent solubilization, as judged from the line widths, the concentrations of $^{15}N$ and $^{14}N$ labels could be determined from such spectra by using computer subtraction of corresponding single-label spectra under identical detergent conditions. The $^{15}N/^{14}N$ label mole ratio was thus obtained with an accuracy of 15–20%. This relatively large uncertainty is due to the double integrations. Lipid phosphorus determination, according to Rouser et al. (1969), was also performed on the same samples so that the mole fraction of each label relative to the lipids could be computed.

## Theory

*Principles of the Spectral Calculations.* $^{15}N$ nitroxides tumbling rapidly in a quasi-isotropic manner give rise to two narrow ESR lines. The latter are intercalated between the three lines which are observed with the classical $^{14}N$ labels. Thus a five-line composite spectrum can be obtained with a mixture of $^{14}N$ and $^{15}N$ spin-labels, each line being easy to assign. Under appropriate conditions electron spin–electron spin interaction occurs. The broadening is accompanied by a decrease in peak intensity, which for narrow lines is more easily measured than a line-width modification. If one can assume that dipole–dipole interactions are minimized because of fast isotropic motion, the broadening is mainly due to Heisenberg spin exchange that occurs between nitroxide radicals. For a mixture of unlike nitrogen isotopes several exchange rates can be defined. We shall use the following notations: $\tau^{-1}_{14,14}$, $\tau^{-1}_{15,15}$, $\tau^{-1}_{14,15}$, and $\tau^{-1}_{15,14}$ are respectively the electron spin exchange rates between $^{14}N$ and $^{14}N$, $^{15}N$ and $^{15}N$, $^{14}N$ and $^{15}N$, and $^{15}N$ and $^{14}N$ nitroxides. $\tau^{-1}_{i,j}$ is also the average probability per unit of time for a given spin-label $^{i}N$ to exchange its electron spin with any of the spin-labels $^{j}N$. Because of the two possible values of the electron spins, only half of the collisions gives rise to an electron spin exchange. However, not all electron spin exchanges affect the spectral line shape: only those events corresponding to a simultaneous exchange of nuclear spin are "efficient events".

Since $\tau^{-1}_{15,14}$ and $\tau^{-1}_{14,15}$ are both proportional to the total number of electron spin exchanges between unlike spin-labels per unit of time, the following condition must be fulfilled:

$$C_{14}\tau^{-1}_{14,15} = C_{15}\tau^{-1}_{15,14}$$

where $C_{14}$ and $C_{15}$ are respectively the concentrations of $^{14}N$ spin-labels and $^{15}N$ spin-labels. $C_{14}$ and $C_{15}$ are also proportional to the total longitudinal magnetization of the corresponding spin-labels: $M_{\circ 14}$ and $M_{\circ 15}$. Thus

$$M_{\circ 14}\tau^{-1}_{14,15} = M_{\circ 15}\tau^{-1}_{15,14}$$

The above equation ensures an equilibrated exchange of magnetization during the electron spin–electron spin interaction taking place between unlike nitroxides. Note that $\tau_{i,j}$ is the average time ellapsed between two processes of electron spin exchange, experienced by a given $^{i}N$ nitroxide encountering $^{j}N$ nitroxides. In practice, $\tau_{i,j}$ is proportional to the average time between molecular collisions of a given $^{i}N$ spin-label with $^{j}N$ labels. Thus, if $^{14}N$ and $^{15}N$ nitroxides are linked to completely equivalent molecules, the following equalities must be satisfied:

$$\tau_{15,14} = \tau_{14,14} \qquad \tau_{14,15} = \tau_{15,15}$$

The important molecular parameter which can be inferred from the spin exchange rate is the nitroxide collision rate. The explicit relationship between spin exchange rates and molecular collision rates will be introduced under Discussion. In this paper we shall assume that spin exchange takes place only if nitroxides actually collide. This is justified because, unlike the dipolar interaction, spin exchange probability decreases exponentially with distance. The experiments should be carried out under conditions which minimize dipole–dipole interaction. Probes undergoing a fast and quasi-isotropic rotational motion fulfill this condition. However, the dipole–dipole interaction is never completely null.

In earlier publications (Bienvenüe et al., 1978; Seigneuret et al., 1981), we have shown that a mixture of $^{14}N$ and $^{15}N$ spin-labeled fatty acids in egg lecithin liposomes can give rise to a five-line pattern with narrow lines. The present section develops the theoretical framework which enables one to simulate the ESR spectra for a mixture of $^{14}N$ and $^{15}N$ fatty acid derivatives incorporated in the same lipid vesicles. Computed spectra are presented and discussed before experimental results. The simulation allows one to find the proper conditions for reaching the best sensitivity. The range of measurable collision rates is thus determined a priori. In addition the computation will allow us to determine the validity of a more approximate, but more convenient, spectral analysis based on peak heights measurements.

A prerequisite to these simulations is a correct representation of the spectra obtained with either $^{14}N$ labels or $^{15}N$ labels alone, without interaction. Several authors have already carried out such calculations for $^{14}N$ labels [see, for example, Gaffney & McConnell (1974)]. The calculation is basically identical for $^{15}N$ labels except that only two resonance lines

are considered. The hypothesis and notations used in the present paper for these simulations are the same as in Davoust & Devaux (1982). Each independent $^{14}N$ spectrum requires six parameters: $T'_{\parallel}$, $T'_{\perp}$, $\Delta H$, $T^{-1}_{2,14}$, $T^{0}_{2,14}$, and $T^{+1}_{2,14}$. $T'_{\parallel}$ and $T'_{\perp}$ are the principal values of the hyperfine tensor of the time-independent effective Hamiltonian; $\Delta H$ gives the shift due to the time averaged $g$ factor anisotropy. $(T^{m}_{2,14})^{-1}$ for $m = 1, 0, -1$ are the line widths. For $^{15}N$ nitroxides, the line widths are $(T^{n}_{2,15})$ with $n = {}^{1}/_{2}, {}^{-1}/_{2}$.

A spectrum corresponding to an isotropic suspension with noninteracting spins is obtained by adding Lorentzian lines. Each Lorentzian triplet, or doublet, is associated with one orientation $\theta_k$ of the bilayer normal. For a fixed field strength $H$, the total contribution of one bilayer orientation can be calculated by solving a set of Bloch equations.

With a $^{14}N$ and $^{15}N$ mixture in the absence of saturation, six equations are associated with $^{14}N$ lines and four equations with $^{15}N$ lines. In the absence of spin interaction, the equations are coupled in pairs and give the Lorentzian line shape when solving for different H values.

Allowing spin–spin interaction means coupling all ten equations. For $^{14}N$ and $^{15}N$ the out-of-phase and in-phase magnetization components, with nuclear spin $m$ and $n$, are respectively $u^{m}_{14}$, $v^{m}_{14}$ and $u^{m}_{15}$, $v^{n}_{15}$. The modified Bloch equations can be written, for each nuclear spin $m$ of the $^{14}N$ labels, as

$$\dot{u}^{m}_{14} + [\omega - \omega^{m}_{14}(\theta_k)]v^{m}_{14} = -[(T^{m}_{2,14})^{-1} + \tau^{-1}_{14,14} + \tau^{-1}_{14,15}]u^{m}_{14} + \frac{1}{3}[\sum_{m'}\tau^{-1}_{14,14}u^{m'}_{14} + \sum_{n'}\tau^{-1}_{15,14}u^{n'}_{15}] \quad (1)$$

$$\dot{v}^{m}_{14} - [\omega - \omega^{m}_{14}(\theta_k)]u^{m}_{14} = -[(T^{m}_{2,14})^{-1} + \tau^{-1}_{14,14} + \tau^{-1}_{14,15}]v^{m}_{14} + \frac{1}{3}[\sum_{m'}\tau^{-1}_{14,14}v^{m'}_{14} + \sum_{n'}\tau^{-1}_{15,14}v^{n'}_{15}] + \gamma H_1 M^{m}_{z14} \quad (2)$$

where $m = -1, 0, 1$. The second term in the right-hand side of eq 1 and 2 corresponds to the efflux of the magnetization from $^{14}N$ and $^{15}N$ labels of any nuclear spin $m'$ and $n'$ toward one nuclear spin $m$ of the $^{14}N$ labels. Since only one-third of the total flux of magnetization reaches each nuclear spin $m$, a factor ${}^{1}/_{3}$ appears in eq 1 and 2.

A similar set of Bloch equations can be written for each nuclear spin $n$ of the $^{15}N$ labels ($n = {}^{-1}/_{2}, {}^{1}/_{2}$). In the latter equations, a factor ${}^{1}/_{2}$ is introduced in place of ${}^{1}/_{3}$ because $^{15}N$ labels have only two possible nuclear spins. Altogether five sets of modified Bloch equations can be written. They are coupled through the $\tau^{-1}_{i,j}$ terms.

The frequency units, used here for convenience, are related to the magnetic field through the relation $\omega = [\gamma/(2\pi)]H$ where $\gamma$ is the gyromatic ratio of the unpaired electron of the nitroxide. $\omega^{m}_{14}(\theta_k)$ represents the position in frequency units of the Lorentzian line with nuclear spin $m$ when the orientation of the membrane is $\theta_k$. For an experiment carried out at a fixed nonsaturant microwave frequency and variable magnetic field in the slow passage limit, $M^{m}_{z14} = M_{\circ 14}/3$ and $M^{n}_{z15} = M_{\circ 15}/2$.

Under steady-state conditions the modified Bloch equation can be solved (see Appendix). The spectrum corresponding to the superposition of all membrane orientations is obtained by an appropriate angular summation.

*Simulated Spectra. Parameterization.* First, we carried out simulations to fit the spectra obtained with either $^{14}N$ or $^{15}N$ spin-labeled fatty acids diluted in egg lecithin liposomes. Experimental spectra were recorded at 35, 45, and 55 °C with samples containing a low concentration of either $^{14}N(1,14)PC$ or $^{15}N(1,14)FA$. After simulation of the diluted spectra, we included the contribution of both isotopes in the same computed spectrum and accounted for electron spin–electron spin

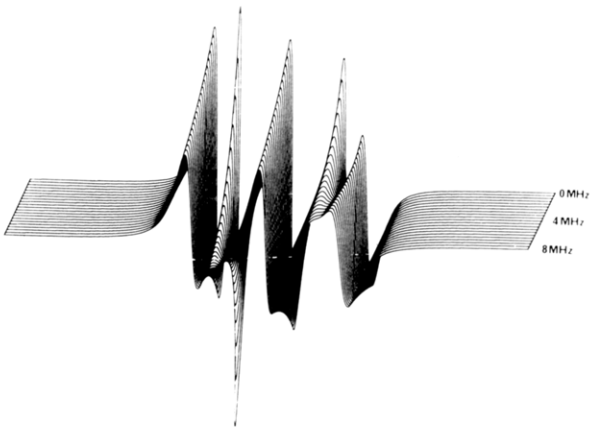


FIGURE 2: Simulated ESR spectra corresponding to a mixture of $^{15}N$ and $^{14}N$ spin-labels. Mole ratio of $^{15}N$ to $^{14}N$: 1 to 4. Spectral parameters (in G): $T'_{\parallel} = 15.16$, $T'_{\perp} = 14.18$, $\Delta H = 0.81$, LW (1) = 1.25, LW(0) = 1.20, and LW(−1) = 1.72 for the $^{14}N$ label; $T'_{\parallel} = 21.80$, $T'_{\perp} = 19.40$, $\Delta H = 0.28$, LW(${}^{1}/_{2}$) = 1.11, and LW(${}^{-1}/_{2}$) = 1.71 for the $^{15}N$ label. The $^{14}N$–$^{14}N$ electron spin exchange frequency is constant: $\tau^{-1}_{14,14} = 3.8$ MHz. Numbers on the right refer to the $^{15}N$–$^{14}N$ electron spin exchange frequency: $\tau^{-1}_{15,14}$ which varies linearly from 0 (rear spectrum) to 8.4 MHz (front spectrum) with 0.42-MHz steps.

interactions by introducing in the calculation finite values for $\tau^{-1}_{ij}$. We paid particular attention to the influence on the spectral line shape of $\tau^{-1}_{14,14}$ and $\tau^{-1}_{15,14}$ while $\tau^{-1}_{15,15}$ was assumed to be negligible. A typical set of spectra is shown in Figure 2, where an ensemble of results corresponding to different values of $\tau^{-1}_{15,14}$ is displayed for a fixed value of $\tau^{-1}_{14,14}$. In this figure, $\tau^{-1}_{14,14} = 3.8$ MHz, which corresponds to approximately 0.04 mol of $^{14}N(1,14)FA$/mol of lipids (at a temperature of 45 °C); $\tau^{-1}_{15,15}$ is set to zero; finally the molar ratio between $^{15}N$ labels and $^{14}N$ labels is 1/4. Spectra are normalized to the same total spin-label concentration. The top spectrum of Figure 2 corresponds to $\tau^{-1}_{15,14} = 0$. This figure illustrates the large effect of heteroisotopic spin exchange on the spectral components corresponding to the minor quantity (here $^{15}N$). The line-shape modifications are visible in a frequency range covering 0.1–10 MHz. In this range the peak height of the narrow low-field line ($n = +{}^{1}/_{2}$) could in fact be used to monitor exchange effects. On the contrary $^{14}N$ lines, which are already broadened by $^{14}N$–$^{14}N$ interactions, are only moderately sensitive to the increasing spin exchange with $^{15}N$ lines, in the same frequency domain.

Changing $\tau^{-1}_{14,14}$ and/or the $^{15}N/^{14}N$ ratio, as well as introducing a finite value for $\tau^{-1}_{15,15}$, leads to a different set of simulated spectra. We have established a certain number of typical sets, and from these, qualitative conclusions can be drawn, which are summarized as follows.

Appreciable sensitivity to $\tau^{-1}_{15,14}$ requires three conditions: (i) resonance peaks of the various isotopes must be clearly distinguishable; (ii) peak heights must vary when $\tau^{-1}_{15,14}$ varies; (iii) a large $^{14}N$ or $^{15}N$ component must not overwhelm the peak sensitive to $\tau^{-1}_{15,14}$.

These conclusions impose in fact experimental conditions close to those chosen in Figure 2. In particular, it is important that one of the isotopes be diluted, if attention is given to low frequencies. It is advantageous to use nitrogen-15 as the dilute isotope because, first, intrinsic line widths are narrower and, second, the intensity is included in two lines, instead of three for $^{14}N$ labels. Thus for a given concentration of spin-label, $^{15}N$ lines are more intense than $^{14}N$ lines. A ratio of $^{15}N$ to $^{14}N$ as low as 0.1 can be used, for small $\tau^{-1}_{15,14}$ values.

In order to describe the results of Figure 2 in a quantitative way, we have measured the magnitude $H$ of the low-field $^{15}N$

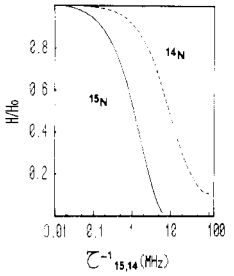


FIGURE 3: Relative intensity decrease of the $^{15}N$ low-field line (solid curve) and of the $^{14}N$ mid-field line (dashed curve) vs. $^{15}N$–$^{14}N$ spin exchange frequency (logarithmic scale) for a 1:4 mixture of $^{15}N$ and $^{14}N$ spin-labels. Data are taken from spectra of Figure 2.

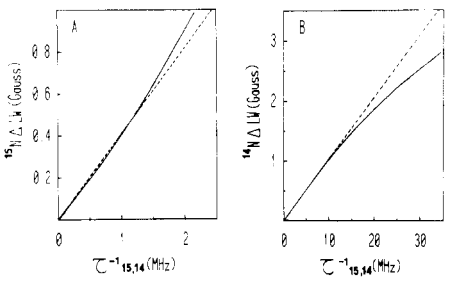


FIGURE 4: Broadening of the $^{15}N$ low-field line (A) and of the $^{14}N$ mid-field line (B) vs. $^{15}N$–$^{14}N$ exchange frequency for a 1/4 mixture of $^{15}N$ and $^{14}N$ spin-labels. Line broadening is calculated from peak height measurements by using eq 3 with the following line widths: $LW_0$ = 1.11 G for the $^{15}N$ low-field line (A) and $LW_0$ = 1.95 G for the $^{14}N$ mid-field line (B). This latter value takes into account the intrinsic line width and the effect of the $^{14}N$–$^{14}N$ electron spin interaction. Data are deduced from spectra of Figure 2.

line ($n = +^1/_2$) and that of the central $^{14}N$ line ($n = 0$). Normalization was obtained by dividing $H$ values by the magnitude $H_0$ of the peaks in the absence of interaction ($\tau^{-1}_{15,14} = 0$). $H/H_0$ for $n = {}^1/_2$ and $m = 0$ was then plotted against $\tau^{-1}_{15,14}$ (Figure 3). This presentation clearly shows in which frequency range the technique is sensitive.

It is possible to relate rather directly the peak height variation to the heteroisotopic spin exchange rate $\tau^{-1}_{15,14}$. Indeed as long as the resonance peaks are still Lorentzian, the peak height can be related to the line width (LW). The increase of line width $\Delta$(LW) is, in turn, proportional to the exchange frequency, at least for low frequencies. Thus, if $LW_0$ is the line width in the absence of interaction

$$\Delta(\mathrm{LW}) = \mathrm{LW}_0(\sqrt{H_0/H} - 1) \qquad (3)$$

is the broadening due to spin exchange. This quantity, as a first approximation, should be proportional to $\tau^{-1}_{15,14}$ and thus should vary linearly with the $^{14}N$ mole fraction for low concentrations of $^{14}N$ spin-label. Parts A and B of Figure 4 show respectively the plots of $^{15}N$ low-field line broadening and $^{14}N$ central line broadening as a function of $\tau^{-1}_{15,14}$. $\Delta$(LW) values are calculated by eq 3 from the simulated spectra of Figure 2. As already mentioned, under the conditions of Figure 2, the appropriate frequency range is different for both probes. The diluted $^{15}N$ labels are more sensitive to lower frequency than the concentrated $^{14}N$ labels. The linear approximation, which is only rigourous near $\tau^{-1}_{15,14} \simeq 0$, is tolerable in the frequency domain 0.05–0.5 MHz for the $^{15}N$ line and 0.5–5 MHz for the $^{14}N$ line.

Note that if the order parameter of one of the probes, $^{15}N$ or $^{14}N$, is high, overlap between lines would occur. Then the plots of $\Delta$(LW) vs. $\tau^{-1}_{15,14}$ would deviate from linearity even for low values of $^{14}N$ mole fraction. Nevertheless the latter plots can always be used for *comparative* purposes.

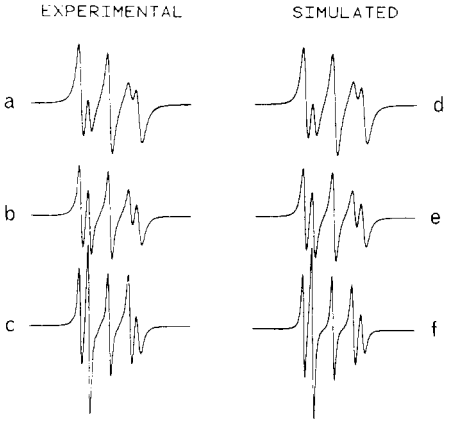


FIGURE 5: (Left) Experimental ESR spectra of mixtures of $^{15}N$-(1,14)FA and $^{14}N$(1,14)PC in egg lecithin liposomes at 45 °C. Mole fraction of $^{15}N$(1,14)FA: 0.010 in all samples. Mole fraction of $^{14}N$(1,14)PC: (a) 0.044, (b) 0.022, and (c) 0.011. Spectra are normalized in amplitude to the same amount of $^{15}N$ label. (Right) Simulated ESR spectra with the following parameters (in G): $T'_{\parallel}$ = 15.16, $T'_{\perp}$ = 14.18, $\Delta H$ = 0.81, LW(1) = 1.25, LW(0) = 1.20, and LW(−1) = 1.72 for $^{14}N$(1,14)PC; $T'_{\parallel}$ = 21.80, $T'_{\perp}$ = 19.40, $\Delta H$ = 0.28, LW($^1/_2$) = 1.15, LW($-^1/_2$) = 1.60 for $^{15}N$(1,14)FA. Exchange frequencies $\tau^{-1}_{14,14}$ and $\tau^{-1}_{15,14}$ (in MHz) are respectively (d) 3.78 and 3.36, (e) 1.68 and 1.95, and (f) 0 and 0.

## Experimental Results

We have carried out a series of experiments using $^{15}N$-(1,14)FA diluted in egg lecithin liposomes. These experiments were done at pH 8; therefore, the fatty acid was likely to be in an ionized form (Egret-Charlier et al., 1978). The liposomes contained, in addition to the $^{15}N$ spin-label, higher concentrations of one of the $^{14}N$ spin-labeled lipids represented in the right part of Figure 1. The goal is to determine the collision rates between probes having a different average position within the hydrophobic core of the membrane.

Particular attention is given to the interactions between $^{15}N$(1,14)FA and $^{14}N$(1,14)PC on the one hand and $^{15}N$-(1,14)FA and $^{14}N$(0,2)PC on the other hand. The advantage of these three molecules lies in the fact that they give rise to narrow ESR lines because of the high mobility of the probes. Under Theory we have emphasized the importance of narrow lines in order to be able to properly simulate the spectra. The interaction of $^{15}N$(1,14)FA with the other $^{14}N$ spin-labels included in Figure 4 will be analyzed solely by peak heights measurements.

The left part of Figure 5 shows a series of spectra recorded at 45 °C. They correspond to mixture of $^{15}N$(1,14)FA and $^{14}N$(1,14)PC in lecithin liposomes. The concentration of nitrogen-15 label is maintained at a level of 1 mol of spin-label/100 mol of phospholipid, while the concentration of nitrogen-14 label is increased in the figure from 2.2% to 7%. All spectra are normalized in amplitude so that a constant amount of $^{15}N$ nitroxide is present. The intensity loss of the $^{15}N$ lines associated with the increase of $^{14}N$(1,14)PC molar fraction is indicative of heteroisotopic spin–spin interaction. Similar results have been obtained between 15 and 55 °C.

The left part of Figure 6 shows experimental spectra obtained with $^{15}N$(1,14)FA in the presence of increasing concentration of $^{14}N$(0,2)PC. Spectra are again normalized with regard to the concentration of $^{15}N$ spin-label. The decrease of intensity of the $^{15}N$ lines is much less pronounced than in Figure 5.

The experimental spectra of Figures 5 and 6 have been computer simulated by the method described under Theory. In Figures 5 and 6 the simulated spectra (on the right) are compared with experimental spectra (on the left). Values of

Table I: Slopes of Exchange Frequencies vs. $^{14}N$ Label Mole Fraction and Apparent Lateral Diffusion Coefficients in Lecithin Liposomes

| labels | | | 35 °C | | 45 °C | | 55 °C | |
|---|---|---|---|---|---|---|---|---|
| $^{15}N$ | $^{14}N$ | | $^{14}N$–$^{14}N$ | $^{15}N$–$^{14}N$ | $^{14}N$–$^{14}N$ | $^{15}N$–$^{14}N$ | $^{14}N$–$^{14}N$ | $^{15}N$–$^{14}N$ |
| (1,14)FA[a] | (0,2)PC | slope[b] (MHz) | 27 ± 11 | 5.6 ± 4.7 | 31 ± 8 | 3.9 ± 0.9 | 27 ± 6 | 5.6 ± 5.6 |
| | | $D_{app}$[c] ($10^{-8}$ cm$^2$ s$^{-1}$) | 2.9 ± 1.2 | 0.6 ± 0.5 | 3.3 ± 0.8 | 0.4 ± 0.1 | 2.9 ± 0.6 | 0.6 ± 0.6 |
| (1,14)FA[a] | (1,14)PC | slope[b] (MHz) | 75 ± 9 | 59 ± 8 | 76 ± 6 | 74 ± 4 | 88 ± 7 | 87 ± 3 |
| | | $D_{app}$[c] ($10^{-8}$ cm$^2$ s$^{-1}$) | 7.9 ± 1.0 | 6.4 ± 0.9 | 8.1 ± 0.6 | 7.9 ± 0.5 | 9.4 ± 0.7 | 9.2 ± 4 |

[a] Mole fraction 0.010. [b] Obtained from plots of $\tau^{-1}_{14,14}$ and $\tau^{-1}_{15,14}$ vs. $^{14}N$ label mole fraction (see Figure 7). Exchange frequencies were obtained from spectral simulations. [c] Apparent lateral diffusion coefficient calculated assuming an hexagonal packing array with three new neighbors at each jump (see Discussion).

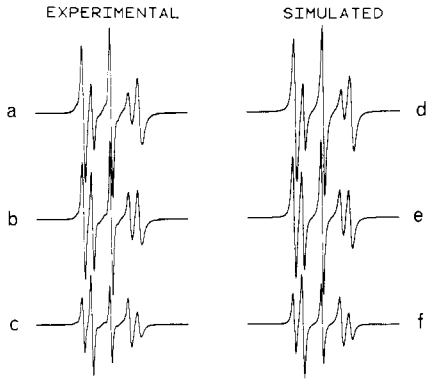


FIGURE 6: (Left) Experimental ESR spectra of mixtures of $^{15}N$-(1,14)FA and $^{14}N$(0,2)PC in egg lecithin liposomes at 45 °C. Mole fraction of $^{15}N$(1,14)FA: 0.010 in all samples. Mole fraction of $^{14}N$(0,2)PC: (a) 0.035, (b) 0.015, and (c) 0.008. All spectra are normalized in amplitude to the same amount of $^{15}N$ label (note that the normalization factor is 3 times less than that of Figure 5). (Right) Simulated ESR spectra with the following parameters (in G): $T'_{\parallel}$ = 15.60, $T'_{\perp}$ = 14.30, $\Delta H$ = 0.17, LW(1) = 1.09, LW(0) = 1.07, and LW(−1) = 1.63 for $^{14}N$(0,2)PC; same as in the legend of Figure 5 for $^{15}N$(1,14)FA. Exchange frequencies $\tau^{-1}_{14,14}$ and $\tau^{-1}_{15,14}$ (in MHz) are respectively (d) 0.42 and 0.08, (e) 0.22 and 0, and (f) 0 and 0.

$\tau^{-1}_{15,14}$ and $\tau^{-1}_{14,14}$ which give the best fit are shown in Figure 7. Several criteria were used to define a good fit: (i) hyperfine splittings, (ii) relative peak heights, (iii) apparent line widths, and (iv) double integral. All relative peak heights can be rigorously measured and were adjusted within 5% maximum error. On the other hand, only the line widths of the $^{14}N$ lines can be significantly evaluated. Thus particular attention was given to the low- and high-field $^{14}N$ line widths. The spectra corresponding to the diluted samples were fitted first; then only the exchange frequencies were allowed to vary when fitting spectra corresponding to a high concentration of label.

A striking diffeence exists between spin exchange frequencies corresponding to Figure 5 and those corresponding to Figure 6. Practically no spin exchange can be measured between $^{15}N$(1,14)FA and $^{14}N$(0,2)PC. Note also that for the same concentration of spin-label the exchange frequency between $^{14}N$(1,14)PC molecules is more than 2 times that measured between $^{14}N$(0,2)PC molecules. Figure 7 indicates that $\tau^{-1}_{14,14}$ and $\tau^{-1}_{15,14}$ can be represented as a function of the mole fraction of $^{14}N$ label by straight lines. The values of the slopes are larger for mixtures containing (1,14)PC than for those containing (0,2)PC. Table I indicates the slopes obtained at 35, 45, and 55 °C. The slopes of such lines are directly proportional to the lateral diffusion constants (see Discussion). Table I indicates the apparent lateral diffusion coefficient calculated assuming the same number of new neighbors at each jump for (1,14)PC and (0,2)PC.

We have also applied the simple analysis based on peak height measurements (see Theory). Figure 8A shows the $^{15}N$ low-field line broadening deduced by peak height measurements on the 45 °C sample containing $^{14}N$ and $^{15}N$ spin-labels,

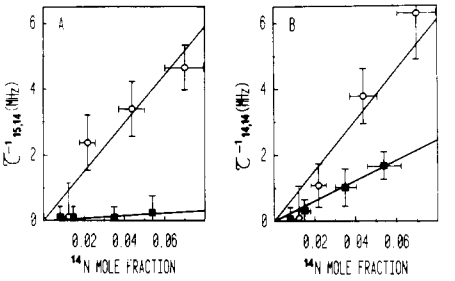


FIGURE 7: $^{15}N$–$^{14}N$ (A) and $^{14}N$–$^{14}N$ (B) exchange frequencies vs. $^{14}N$ label mole fraction for mixtures of $^{15}N$(1,14)FA (constant mole fraction 0.010) and $^{14}N$(1,14)PC (○) or $^{14}N$(0,2)PC (■) in lecithin liposomes at 45 °C. Exchange frequencies were obtained from simulations of the corresponding ESR spectra (see Figures 5 and 6). Vertical error bars result mostly from the uncertainty in the $^{15}N/^{14}N$ label mole ratio which has been taken into account in the simulations but also from the fact that different values give reasonable fits (systematic errors).

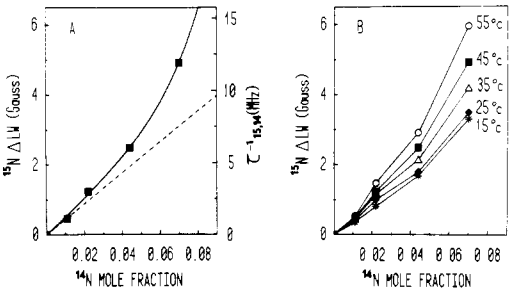


FIGURE 8: (A) $^{15}N$ label low-field line broadening vs. $^{14}N$ label mole fraction for mixtures of $^{15}N$(1,14)FA (constant mole fraction 0.010) and $^{14}N$(1,14)PC in egg lecithin liposomes at 45 °C (■). Line broadening expressed in gauss (left scale) were calculated from peak height measurements by using eq 3 with an intrinsic line width $LW_0$ = 1.11 G. Data were fitted to a fourth-order polynomial (solid curve) by using a nonlinear least-squares program. The tangent at origin (dashed line) gives a rough estimate of $\tau^{-1}_{15,14}$ expressed in megahertz (right scale) to be compared with Figure 7A. (B) Same results at various temperatures. Intrinsic line widths $LW_0$ used in the calculations were respectively from 15 to 55 °C (in G) 1.30, 1.16, 1.15, 1.11, and 1.07. Vertical error bars varying from 0.2 to 1 G have been omitted for clarity.

each label being at the $\omega - 2$ position. The slope at the origin is determined in order to obtain the best estimate of $\tau^{-1}_{15,14}$ (see Theory). Figure 8B shows that the broadening and hence the exchange frequency increase with temperature. Figure 9 shows the spectra of $^{15}N$(1,14)FA in the presence of increasing concentration of either $^{14}N$(10,3)PC or $^{14}N$(7,8)FA. Figure 10A contains the results for the interaction of $^{15}N$(1,14)FA with all the spin-labels included in Figure 1. As can be seen, broadening of the $^{15}N$(1,14)FA low-field line becomes less and less important as the $^{14}N$ nitroxide is moved up in position along the fatty acid chain. Figure 10B shows how the results are modified if the $^{15}N$ label is linked to an ester molecule instead of an ionized fatty acid. In this latter experiment, the broadening fails to discriminate between the different spin-

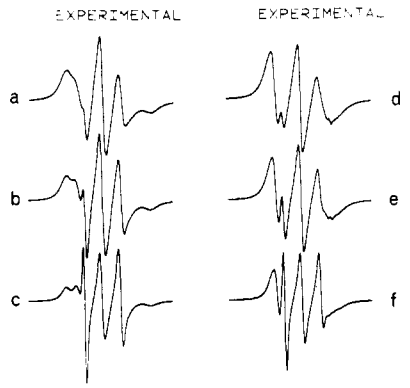


FIGURE 9: Experimental ESR spectra of mixtures of $^{15}$N(1,14)FA with $^{14}$N(10,3)PC (a, b, c) and $^{14}$N(7,8)FA (d, e, f) in egg lecithin liposomes at 45 °C. Mole fraction of $^{15}$N(1,14)FA: 0.01 in all samples. Mole fraction of $^{14}$N label: (a) 0.063, (b) 0.026, (c) 0.017, (d) 0.073, (e) 0.048, and (f) 0.026. Spectra are normalized in amplitude to the same amount of $^{15}$N label.

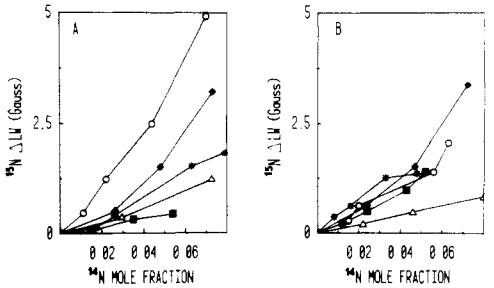


FIGURE 10: $^{15}$N low-field line broadening vs. $^{14}$N label mole fraction for mixtures of (A) $^{15}$N(1,14)FA or (B) its methyl ester (constant mole fraction 0.010) with various $^{14}$N lipid spin-labels: $^{14}$N(1,14)PC (○), $^{14}$N(7,8)FA (♦), $^{14}$N(10,3)PC (*), $^{14}$N(0,2)PC (■), and [$^{14}$N]tempolecithin (▲) in egg lecithin liposomes at 45 °C. Line broadening was calculated from peak height measurements by using eq 3 with an intrinsic line width $LW_0$ = 1.11 G for both labels. Vertical error bars varying from 0.2 to 1 G have been omitted for clarity.

labeled lipids. However, tempolecithin (TL), which bears a nitroxide on the polar head group, does not interact with either (1,14)FA or (1,14) ester.

## Discussion

*Spectral Simulations and Determination of the Spin Exchange Rates* ($\tau_{i,j}^{-1}$). First we consider the validity of the spectral simulations. Fitting the spectra of the diluted samples, for which spin–spin interactions can be neglected, requires the introduction of six independent parameters for the $^{14}$N lines and five independent parameters for the $^{15}$N lines. One approximation used in this paper (intrinsic line width independent of orientation) limits the number of parameters but precludes the simulation of spectra corresponding to spin-labels with high order such as (10,3)PC. See, for example, Gaffney & McConnell (1974). On the other hand a good fit can be obtained, particularly at high temperature, with spin-labels (1,14)PC and (0,2)PC. When the spin–spin interaction is taken into account two new parameters are introduced, namely, $\tau_{15,14}^{-1}$ and $\tau_{14,14}^{-1}$. These new parameters, within the framework of modified Bloch equations, allowed us to perform good fits of the spectra corresponding to samples containing a high concentration of $^{14}$N label (see Figures 5 and 6). Good fits were obtained at 55, 45, and 35 °C but not at lower temperatures. These results prove that Heisenberg spin exchange is the dominant broadening mechanism at high temperature, i.e., under conditions of low viscosity. The poor fit observed at low temperature (high viscosity) can be attributed to the neglect of dipole–dipole interaction. Devaux et al. (1973) and Hyde & Sarna (1978) have also reported that the contribution of the dipole–dipole interaction to the broadening is dominant when the sample viscosity is high, whereas spin exchange is dominant for low viscosity samples.

The spectral analysis deduced from peak height measurements appears in Figures 8 and 9. The peak height variation is converted into line-width variation, Δ(LW), which in turn can be converted into a spin exchange rate (see Theory). Comparison with the results of complete spectral simulations shows that if Δ(LW) is expressed in megahertz, through the use of eq 3, $\tau_{15,14}^{-1}$ and $\tau_{14,14}^{-1}$ are overestimated for large values of the $^{14}$N mole fraction. This is due partly to the overlap between $^{14}$N and $^{15}$N lines and is consistent with the nonlinearity of Δ(LW) vs. $\tau_{i,j}^{-1}$ appearing in Figure 4. Nevertheless this simple treatment allows one to obtain very rapidly approximate values of $\tau_{15,14}^{-1}$. Particular attention should be given to the initial slope of Δ(LW) vs. $^{14}$N mole fraction if absolute measurements of $\tau_{15,14}^{-1}$ are necessary. On the other hand, if only relative values are required, fruitful comparisons can be obtained for large values of the $^{14}$N mole fraction (see Figures 8 and 9).

*Relation between the Electron Spin Exchange Rates and the Molecular Collision Rates.* We assume the Heisenberg spin exchange interaction to be of sufficiently short range that the exchange interaction is only effective when two oxazolidine rings are essentially in van der Waals contact. Within a model of rapid diffusion, the interaction time between nitroxides is short ($\lesssim 10^{-7}$ s), and one can admit that a single-exchange process can take place at each collision. The number of collisions per unit of time of a given $^{i}$N label with any $^{14}$N label is $2\tau_{i,14}^{-1}$, where $i$ is either 14 or 15 (see Theory). In the range of spin-label concentration used in this study (mole fraction of $^{14}$N label $\lesssim$7%), we have found that $\tau_{i,14}^{-1}$ is proportional to the molar fraction of $^{14}$N spin-label (see Figure 7). We can write

$$2\tau_{i,14}^{-1} = \nu(C_{14}/C_{\text{lip}})$$

where $C_{14}/C_{\text{lip}}$ is the molar fraction of spin-labeled lipids and $\nu$ a parameter which is deduced from the slope of $\tau_{i,14}^{-1}$ when represented as a function of $^{14}$N mole fraction (see Table I).

What is the physical meaning of $\nu$ for a given experiment? Let us extrapolate to a mole fraction of 1.[2] Then

$$2(\tau_{i,j}^{-1})_{\text{limit}} = \nu$$

is the frequency with which a nitroxide $^{i}$N collides with new neighbor nitroxides (all of them being $^{14}$N type). Assuming a hopping model on a *fixed* lattice and a number of new neighbor sites after each jump equal to $m$, then $f = \nu/m$ is the hopping frequency of a lipid $^{i}$N. Note that $m$ depends upon the type of spin-labels interacting and does not represent the mere number of neighbor phospholipids. From $f$ and from the average distance $a$ between neighbor lipids, one can deduce the rate of lateral diffusion and hence the diffusion constant $D$. Namely[3]

$$D = \frac{a^2 f}{\theta} = \frac{a^2}{\theta}\frac{\nu}{m} \qquad (4)$$

[2] Even with a molar fraction of $^{14}$N equal to 1, it is tolerable to allow $i$ to be either 14 or 15.

[3] Equation 4 is a simplified version of the formula proposed by Sackmann and Traüble in 1972 to deduce the diffusion constant from the spin exchange rate. Both equations are close, if the mole fraction is small. The coefficient $m$ that we have introduced in eq 4 allows a variation of the effective interaction diameter of the radicals. This was a parameter introduced explicitly by Sackmann and Traüble.

$\theta$ is a numerical factor which includes the dimensionality of the diffusion process and also takes into account the fact that each collision takes place between two *mobile* molecules. In the present situation we find $\theta = 8$. Note that if one of the paramagnetic species is prevented from diffusion, for example, because it is linked to a protein, then $\theta = 4$ [Davoust et al. (1983)]. Previous calculations which led to the diffusion constant of lipids from analysis of the Heisenberg spin exchange ignored the difference between the two above situations and hence overestimated $D$ by a factor of 2 (Devaux et al., 1973; Sackmann & Traüble, 1972b).

How does one determine $m$? It has been assumed in former work (Devaux et al., 1973) (i) that phospholipids diffuse in a regular hexagonal array and (ii) that electron spin exchange takes place only between close neighbor phospholipids. These two hypotheses led to $m = 3$. Table I contains the values of the apparent diffusion constants of (1,14)PC and (0,2)PC molecules diluted in egg lecithin, as deduced from eq 4 with $m = 3$. Note that significantly different values of $D$ are obtained for the two spin-labeled lipids. However, $m = 3$ may be an oversimplification when the label is attached near the methyl terminal of a fatty acid chain, (1,14)PC. In such position, the probability of contact with a second closest neighbor may be different from zero and $m$ larger than 3. Thus if the lateral diffusion rate ($f$) is known, $m$ should be considered as the unknown parameter and deduced from these experiments.

Up to now, the discussion implicitly assumed that a molecular collision between spin-labeled phospholipids automatically corresponds to a collision between nitroxides. This is a safe assumption for equivalent spin-labels, but not for a collision between two different spin-labeled lipids, for example, $^{15}N$(1,14)FA and $^{14}N$(0,2)PC. In such a case a molecular collision does not imply that nitroxides come in close contact. Thus we can write formally

$$\nu = Pmf \qquad 0 < P < 1$$

$P$ is a probability factor whose value is taken as 1 for a collision between equivalent spin-labels and 0 for a collision between two spin-labels such as (1,14)FA and (0,2)PC. Note that $P$ depends upon the relative position of the labels $^{l}N$ and $^{14}N$ along the labeled fatty acid chains, also upon the flexibility of the labeled residues, and hence upon the spatial domains swept by each nitroxide.

This decomposition of $\nu$ into the product of three terms is somewhat arbitrary. $P$ and $m$ could be combined in a single "overlap integral". However, the present decomposition emphasizes that one contribution to the overlap integral is due to the size of the area swept by each nitroxide in a plane parallel to the plane of the membrane ($m$) while a second contribution comes from the depth of the probe within the membrane ($P$).

*What Are the New Pieces of Information Obtained Concerning the Motion of Spin-Labeled Lipids?* (*a*) *Collisions between Like Spin-Labels.* Table I shows the "apparent diffusion constants" which have been calculated, according to eq 4, from the slopes of the spin exchange rates plotted against the mole fraction of $^{14}N$ label and assuming $m = 3$. The values obtained with the two spin-labeled phospholipids differ in magnitude. Of course (0,2)PC is a molecule different from (1,14)PC, and a different rate of lateral diffusion could be invoked. But this is unlikely since lateral diffusion is not very sensitive to molecular size. It must be concluded that the spin exchange is more efficient within (1,14)PC molecules than within (0,2)PC molecules and $m$ (the average number of new neighbor nitroxides at each molecular jump) must be different for (1,14)PC and for (0,2)PC. We postulate that, because of the small size of the $\beta$ chain of (0,2)PC, the probe on this latter molecule interacts magnetically only with labeled phospholipids in direct contact. Thus $m = 3$ for a mixture of (0,2)PC spin-labels, and since $m = 3$ was used in Table I to obtain the diffusion constants through eq 4, adequate values of $D$ are obtained for (0,2)PC at all temperatures.

If $D$ is the same for (1,14)PC and (0,2)PC, then $m \neq 3$ for collisions between (1,14)PC molecules. From the ratios of the apparent diffusion constants given in Table I, an average value of $m \approx 7$ is obtained for a mixture of (1,14)PC molecules. This values of $m$ implies that a probe at the 16th position of a stearic acid explores more than one layer of lipids corresponding to the closest neighbors. However, less than two complete layers of lipids are "seen" by the probe. Indeed when comparing with (0,2)PC, it appears that the interacting area of (1,14)PC, at 45 °C, is about 2.5 times larger; thus the radius of interaction is multiplied by $(2.5)^{1/2}$. This remark is important for the discussion of the following paper (Davoust et al., 1983).

One can ask if, in fact, the larger value of $D_{apparent}$ obtained with (1,14)PC may not be due to the possible interaction betwen probes situated in two different leaflets. After all, (1,14)PC is capable of interacting with (7,8)FA. The distance between two (1,14)PC probes belonging to two different leaflets is not larger. Yet, because of the folding of the chain, a (1,14)PC probe can interact occasionally by direct contact with a (7,8)FA probe. This is not possible for two (1,14)PC probes belonging to two different leaflets. Thus, to be consistent with our assumption that only direct contacts allow spin exchange, we must rule out the interaction between two sides of a bilayer, namely, $P = 0$ for the interaction between two (1,14)PC's belonging to different leaflets.

(*b*) *Collisions between Unlike Spin-Labels.* Figure 7 shows that the calculated spin exchange frequencies, $\tau^{-1}_{15,14}$ and $\tau^{-1}_{14,14}$, are identical, within error bars, for liposomes containing a mixture of $^{15}N$(1,14)FA and $^{14}N$(1,14)PC. This result implies that the two nitroxides are on equivalent molecules, since the probability of collision of a given $^{15}N$ label with a $^{14}N$ label is identical with that of a given $^{14}N$ label with another $^{14}N$ label. Thus, one can conclude first that the position of an ionized fatty acid in the bilayer is very close to that of a chain included in a phospholipid and second that the lateral diffusion rate of these two molecules is the same. Figure 7 and Table I show also that $\tau^{-1}_{15,14}$ differs from $\tau^{-1}_{14,14}$ for a mixture of $^{15}N$(1,14)FA and $^{14}N$(0,2)PC. In fact $\tau^{-1}_{15,14} \approx 0$, in the latter case. Thus in spite of the low order parameter of a probe linked near the $\omega - 2$ terminal of a fatty acid chain, the bending of the chain does not allow the interaction of the hydrophobic terminal part with the polar head group region.

Figure 9A confirms the large difference of magnetic interaction, and hence of collision rate, between probes at the same position along an alkyl chain and probes at unequivalent positions. The results obtained with (10,3)PC and (7,8)FA are, as expected, intermediate between those obtained with (1,14)PC on the one hand and (0,2)PC or TL on the other hand. In this figure $^{14}N$(10,3)PC appears to interact more strongly with $^{15}N$(1,14)FA than $^{14}N$(0,2)PC does. A difference in overlap integral ($P$) would imply that the probe on (0,2)PC sweeps the more polar region. However, this difference is probably exaggerated by dipole–diple interactions which are less averaged out with (10,3)PC than with (0,2)PC.

In summary a probe attached at the $\omega - 2$ position of a stearic fatty acid chain explores a significant volume around its average position but collides with a very low probability with a probe attached near the head-group region. This finding

is consistent with earlier observations made by Godifici & Landsberger (1974). The latter authors used spin-labeled fatty acids incorporated into liposomes and watched the $^{13}C$ NMR lines of the lipids.

Figure 9B shows a more surprising result. In this figure, it appears that all spin-labels except tempolecithin (TL) interact in an equivalent manner with the $^{15}N(1,14)$ ester. In addition the amount of interaction between $^{15}N(1,14)$ ester and $^{14}N(1,14)PC$ is approximately half that between the acid and the phospholipid. This suggests that the ester molecule is not so well positioned in the membrane as the corresponding ionized fatty acid, due to its hydrophobicity. The result would be consistent, with a rapid flip-flop of the ester within the membrane. Hence spin-labeled fatty acids but not the corresponding esters can be used as molecular dipsticks to investigate the penetration of other labeled compounds in a membrane such as a lipid or a protein.

## Conclusions

This study demonstrates that the use of a mixture of nitrogen-14 and nitrogen-15 spin-labels incorporated into the same membrane can be useful for the investigation of collision rates between specific residues. Two types of information can be obtained: (i) proximity between labeled residues and (ii) approximate rates of lateral diffusion.

This investigation emphasizes the difficulty of measuring the rate of lateral diffusion from collision rates when nonrigid molecules are used. In the absence of independent knowledge of the effective interaction diameter of radicals attached to a phospholipid acyl chain only approximate values of $D$ can be reached (Devaux et al., 1973). On the other hand since many independent measurements of $D$ are now available in the literature, we think that the most fruitful information gained by the present analysis concerns an estimation of the range of the wobbling motion experienced by the different parts of an acyl chain. We find that the amplitude of this motion increases from the head-group region to the methyl-terminal region and increases with temperature. This finding is not to be confused with the classical results concerning the order parameters, since order parameters are not related to the amplitude of the motion.[4] On the other hand, the increase with temperature of the amplitude of the motion of acyl chain was predicted recently by Davoust & Devaux (1982), from a line-shape analysis of spin-labeled fatty acid chains attached to rhodopsin.

The advantage of heteroisotopic labeling is that if A and B type molecules are mixed, by this technique the interactions between A and B molecules can be unambiguously distinguished from interactions between A and A or between B and B. This would not be possible by homogeneous labeling ($^{14}N$–$^{14}N$). In addition components A and B can be at very different ratios; for example, B can be 10 times less concentrated than A and nevertheless be clearly distinguishable. Complete spectral simulations allow the quantitative determination of spin exchange rates and hence of collision rates. The simulations developed in this paper are only accurate if the local motion of the probes is high. This limits the application to high temperature for lipids and to probes weakly bound to proteins. However, qualitative results can be obtained for more restricted motions. In particular the method can be extremely valuable if used on a comparative level. Recently Popp & Hyde (1982) used ELDOR to determine Heisenberg spin exchange frequency between spin-labeled fatty acids. They showed that the mole fraction of spin-label can be extremely low by this method. However, the absolute concentration of spin-label in their sample is about 100 times larger than that necessary for conventional ESR.

The double labeling with nitroxides has the disadvantage of involving the synthesis of specific probes. However, it is in principle a very general technique. To some extent, it is comparable to studies based on the analysis of spectral perturbation produced by a nitroxide on NMR spectra (Kornberg & McConnell, 1971b; Godifici & Landsberger, 1974) or on fluorescence spectra (Haigh et al., 1979; London & Feigenson, 1981). Over the first method ESR has the advantage of a better sensitivity, and it is also adapted to higher frequencies. Comparisons with fluorescent studies involving a nitroxide will be further discussed in the following paper (Davoust et al., 1983) which is devoted to the topic of lipid–protein interaction.

## Acknowledgments

We thank Drs. Edith Favre and Pierre Fellmann for help during the organic syntheses.

## Appendix

*Solution of Bloch Equations.* As mentioned above, the effect of the spin exchange on the overall resonance line shape is treated theoretically by using five sets of modified Bloch equations for each orientation $\theta_k$ of the normal of the bilayer with respect to the magnetic field direction. The final spectrum is obtained by adding the contribution of each orientation $\theta_k$.

For an experiment carried out at a fixed nonsaturant microwave frequency and variable magnetic field in the slow passage limit, we use the following complex notation:

$$\hat{M}^m_{14} = u^m_{14} + iv^m_{14} \qquad \hat{M}^n_{15} = u^n_{15} + iv^n_{15}$$

$$\mathcal{L}^m_{14} = [(T_{2,14})^{-1} + \tau^{-1}_{14,14} + \tau^{-1}_{14,15} - i[\omega - \omega^m_{14}(\theta_k)]]^{-1}$$

$$\mathcal{L}^n_{15} = [(T_{2,15})^{-1} + \tau^{-1}_{15,15} + \tau^{-1}_{15,14} - i[\omega - \omega^n_{15}(\theta_k)]]^{-1}$$

In the steady-state condition $\dot{\hat{M}}_{15} = \dot{\hat{M}}_{14} = 0$; the modified sets of Bloch equations—see eq 1 and 2 for nitrogen-14 spin-label and similar equations for nitrogen-15 spin-label—can be written in the following form:

$$\hat{M}^{m'}_{14} = \frac{1}{3}\mathcal{L}^{m'}_{14}\left(\sum_m \tau^{-1}_{14,14}\hat{M}^m_{14} + \sum_n \tau^{-1}_{15,14}\hat{M}^n_{15} + i\gamma H_1 M_{\circ 14}\right) \quad \text{(A1)}$$

$$\hat{M}^{n'}_{15} = \frac{1}{2}\mathcal{L}^{n'}_{15}\left(\sum_n \tau^{-1}_{15,15}\hat{M}^n_{15} + \sum_m \tau^{-1}_{14,15}\hat{M}^m_{14} + i\gamma H_1 M_{\circ 15}\right) \quad \text{(A2)}$$

We sum eq A1 for $m' = 1, 0, -1$ and eq A2 for $n' = {}^1/_2, -{}^1/_2$:

$$\left(\sum_m M^m_{14}\right)\left(1 - \tau^{-1}_{14,14}\frac{\sum_m \mathcal{L}^m_{14}}{3}\right) - \tau^{-1}_{15,14}\frac{\sum_m \mathcal{L}^m_{14}}{3}\left(\sum_n M^n_{15}\right) = i\gamma H_1 M_{\circ 14}\frac{\sum_m \mathcal{L}^m_{14}}{3} \quad \text{(A3)}$$

$$\left(\sum_n M^n_{15}\right)\left(1 - \tau^{-1}_{15,15}\frac{\sum_n \mathcal{L}^n_{15}}{2}\right) - \tau^{-1}_{14,15}\frac{\sum_n \mathcal{L}^n_{15}}{2}\left(\sum_m M^m_{14}\right) = i\gamma H_1 M_{\circ 15}\frac{\sum_n \mathcal{L}^n_{15}}{2} \quad \text{(A4)}$$

It is convenient to use the more compact notation

[4] Note that (0,2)PC and (1,14)PC have approximately the same low order parameter, yet these two probes have different motional amplitude. Also (1,14)FA in the ionized form has the same order parameter as the (1,14) ester, yet the amplitude of the motions of the two probes is quite different.

$$\hat{M}_{14} = \sum_m \hat{M}^m_{14} \qquad \hat{M}_{15} = \sum_n \hat{M}^n_{15}$$

$$\mathcal{L}_{14} = \left(\sum_m \frac{\mathcal{L}^m_{14}}{3}\right)\left(1 - \tau^{-1}_{14,14}\frac{\sum_m \mathcal{L}^m_{14}}{3}\right)^{-1}$$

$$\mathcal{L}_{15} = \left(\sum_n \frac{\mathcal{L}^n_{15}}{2}\right)\left(1 - \tau^{-1}_{15,15}\frac{\sum_n \mathcal{L}^n_{15}}{2}\right)^{-1}$$

The analytical solution of eq A3 and A4 is given by

$$\hat{M}_{14} + \hat{M}_{15} = i\gamma H_1 \times \frac{M_{\circ 14}\mathcal{L}_{14} + M_{\circ 15}\mathcal{L}_{15} + (M_{\circ 14}\tau^{-1}_{14,15} + M_{\circ 15}\tau^{-1}_{15,14})\mathcal{L}_{14}\mathcal{L}_{15}}{1 - \tau^{-1}_{14,15}\tau^{-1}_{15,14}\mathcal{L}_{14}\mathcal{L}_{15}} \tag{A5}$$

Equation A5 corresponds to the solution of five sets of Bloch equations for a single membrane orientation ($\theta_k$). The absorption corresponding to the superposition of all membrane orientations is obtained by an appropriate angular summation of the imaginary part of $M_{14} + M_{15}$. The latter includes the angular-dependent vaiables $\omega^m_{14}(\theta_k)$ and $\omega^n_{15}(\theta_k)$.

For nonoriented membrane suspension, the angular density probability is isotropic. The contribution to eq A5 of an angular mesh $\Delta\theta$ centered around $\theta_k$ is proportional to (sin $\theta_k)\Delta\theta$. This angular summation was carried out for each magnetic field value and differentiated in order to give the classical first-derivative presentation of EPR spectra. Computation of a single spectrum (600 points for the magnetic field, 20 angular meshs) takes 4 min with a Tektronix 4052.

The program is available under request.

**Registry No.** $^{15}N$(1,14)FA, 69633-15-4; (1,14)PC, 63321-67-5; (7,8)FA, 50613-98-4; (10,3)PC, 55402-85-2; (0,2)PC, 85284-79-3; TL, 68528-86-9.

## References


Berliner, L. J. (1976) *Spin Labeling—Theory and Applications*, Vol. 1, Academic Press, New York.

Bienvenüe, A., Hervé, P., & Devaux, P. F. (1978) *C. R. Hebd. Seances Acad. Sci., Ser. A 287*, 1247–1250.

Davoust, J., & Devaux, P. F. (1982) *J. Magn. Reson. 48*, 475–494.

Davoust, J., Seigneuret, M., Hervé, P., & Devaux, P. F. (1983) *Biochemistry* (following paper in this issue).

Devaux, P., & McConnell, H. M. (1972) *J. Am. Chem. Soc. 94*, 4475–4481.

Devaux, P., Scandella, S. J., & McConnell, H. M. (1973) *J. Magn. Reson. 9*, 474–485.

Devaux, P. F., Bienvenüe, A., Lauquin, G., Brisson, A. D., Vignais, P. M., & Vignais, P. V. (1975) *Biochemistry 14*, 1272–1280.

Egret-Charlier, M., Sanson, A., Ptak, M., & Bouloussa, O. (1978) *FEBS Lett. 89*, 313–316.

Gaffney, B. J., & McConnell, H. M. (1974) *J. Magn. Reson. 16*, 1–28.

Godifici, P., & Landsberger, F. R. (1974) *Biochemistry 13*, 362.

Haigh, E. A., Thulborn, K. R., & Sawyer, W. H. (1979) *Biochemistry 18*, 3525–3532.

Hartmann, W., & Galla, H. J. (1978) *Biochim. Biophys. Acta 509*, 474–490.

Hubbell, W. L., & McConnell, H. M. (1971) *J. Am. Chem. Soc. 93*, 314–326.

Hyde, J. S., & Sarna, T. (1978) *J. Chem. Phys. 68*, 4439–4447.

Kokorin, A. I., Zamarayev, K. I., Grigoryan, G. L., Ivanov, V. P., & Rozantsev (1972) *Biophys. (Engl. Transl.) 17*, 31–39.

Kornberg, R. D., & McConnell, H. M. (1971a) *Biochemistry 10*, 1111–1120.

Kornberg, R. D., & McConnell, H. M. (1971b) *Proc. Natl. Acad. Sci. U.S.A. 68*, 2564–2568.

London, E., & Feigenson, G. W. (1981) *Biochemistry 20*, 1939–1948.

Ohnishi, S. I., & Tokutumi, S. (1981) in *Biological Magnetic Resonance* (Berliner, L., & Reuben, J., Eds.) Vol. 3, pp 121–153, Plenum Press, New York.

Popp, C. A., & Hyde, J. S. (1982) *Proc. Natl. Acad. Sci. U.S.A. 79*, 2559–2563.

Rouser, G., Fleischer, S., & Yamamoto, A. (1969) *Lipids 5*, 494–496.

Sackmann, E., & Traüble, H. (1972a) *J. Am. Chem. Soc. 94*, 4482–4491.

Sackmann, E., & Traüble, H. (1972b) *J. Am. Chem. Soc. 94*, 4492–4498.

Sackmann, E., Traüble, H., Galla, H. J., & Overath, P. (1973) *Biochemistry 12*, 5360–5368.

Scandella, S. J., Devaux, P., & McConnell, H. M. (1972) *Proc. Natl. Acad. Sci. U.S.A. 69*, 2056–2060.

Seigneuret, M., Davoust, J., Hervé, P., & Devaux, P. F. (1981) *Biochimie 63*, 867–870.

Singleton, W. S., Gray, M. S., Brown, M. L., & White, J. L. (1965) *J. Am. Oil Chem. Soc. 42*, 53.